Kelvin Helmholtz Instability in Strongly Coupled Yukawa Liquids

Ashwin J. and R. Ganesh*
Institute For Plasma Research, Bhat, Gandhinagar-382428, India
(Received 9 February 2010; published 27 May 2010)

Using "first principles" molecular dynamics simulations Kelvin Helmholtz instability has been observed for the first time at the particle level in two-dimensional strongly coupled Yukawa liquids. At a given coupling strength Γ a subsonic shear profile is superposed on an equilibrated Yukawa liquid and instability is observed. Linear growth rates computed directly from MD simulations are seen to increase with strong coupling. Vortex-roll formation in the nonlinear regime is reported.

DOI: 10.1103/PhysRevLett.104.215003 PACS numbers: 52.27.Lw, 05.10.−a, 52.65.Yy

A wide variety of physical systems such as complex plasmas, charged colloidal suspensions, and astrophysical white dwarf interiors exist in a state of strong coupling wherein the average potential energy per particle dominates the average kinetic energy [1,2]. It was discovered some years ago that complex plasmas can exist in "liquid" and "crystalline phases" [3–5]. Following this, various authors [6,7] have explored phase transition phenomena using molecular dynamics (MD) simulations. Complex plasmas can behave as essentially single phase systems when the interactions between dust grains dominate over interactions with the background medium [8]. Thus they offer a perfect test bed for numerous flow related studies [9,10]. Some of earliest flow studies were done by D'Angelo [11] who investigated the effect of static charged grains on the stability of magnetized plasma flow. Recently Birk [12] and Wiechen [13] used the conventional two fluid model and investigated the stabilizing effect of dust mass and charge on Kelvin Helmholtz (KH) dust modes. As is well known, for strongly coupled liquids, kinetic theories, let alone their conventional hydrodynamic derivatives suffer from convergence and closure problems [14,15]. To overcome these issues, memory dependent viscoelastic models [16] have been proposed which attempts to describe strongly coupled Yukawa liquids. However, the validity of these models across a wide range of screening parameter and coupling strength is still an open problem [17,18]. Hence in order to correctly describe these systems it becomes imperative to invoke "first principles" MD simulations which amounts to numerically solving the N-body problem "exactly." In the past, MD simulations on short ranged Lennard-Jones systems have been carried out to obtain crucial insights into the onset, growth, nonlinear saturation, and transition to turbulence in Rayleigh-Taylor [19] and Rayleigh-Bennard [20] instabilities.

In this Letter we present one such study of KH instability in a two-dimensional (2D) strongly coupled Yukawa liquid for a step shear profile. For this purpose we use a Yukawa potential given by $\phi(r) = [Q^2/(4\pi\epsilon_0 r)]\exp(-r/\lambda_D)$. Such Yukawa liquids can be fully characterized by two dimensionless parameters: (i) the coupling parameter $\Gamma = Q^2/(4\pi\epsilon_0 a k_B T)$, where Q is the charge of the particles, a is the Wigner-Seitz radius, and (ii) the screening parameter $\kappa = a/\lambda_D$. λ_D is the Debye radius of the background plasma. We use normalized units throughout this Letter. The length, time, and energy are normalized to a, $\omega_{\rm pd}^{-1}$ and $Q^2/(4\pi\epsilon_0 a)$, respectively, where $\omega_{\rm pd} = [Q^2 n/(2\epsilon_0 m a)]^{1/2}$, n and m are the areal number density and mass of particles, respectively. For a given step shear profile and coupling parameter ranging from $\Gamma = 1$ (weak coupling) to $\Gamma = 100$ (strong coupling), we obtain linear growth rates directly from MD simulations and observe nonlinear saturation and vortex-roll formation. It should be noted that for an undriven (flowless) Yukawa system crystallization occurs around $\Gamma \approx 140$ at $\kappa = 0.5$ [21].

MD simulations.—We have performed large scale MD simulations on a 2D system of 2.5×10^5 particles interacting via Yukawa potential. Periodic boundary conditions are employed along $\hat{x}$ and $\hat{y}$. The number density of system n is 0.61, which gives us a square region of size $L = 640$. The value of screening parameter κ in all our simulations is 0.5. The initial state is prepared by first connecting the system

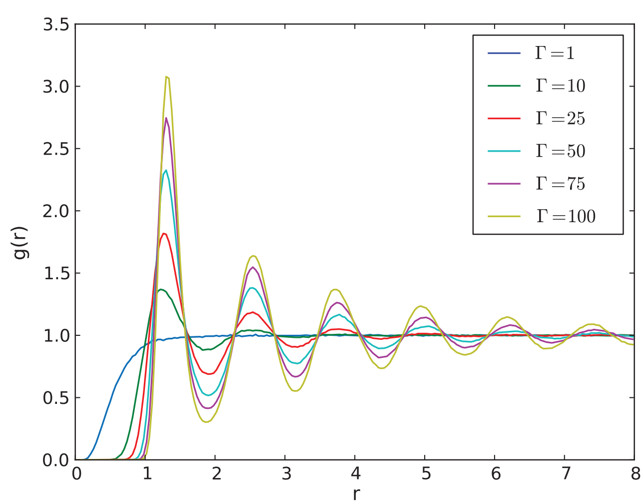

FIG. 1 (color). PCF vs r. Higher values of Γ show stronger coupling.

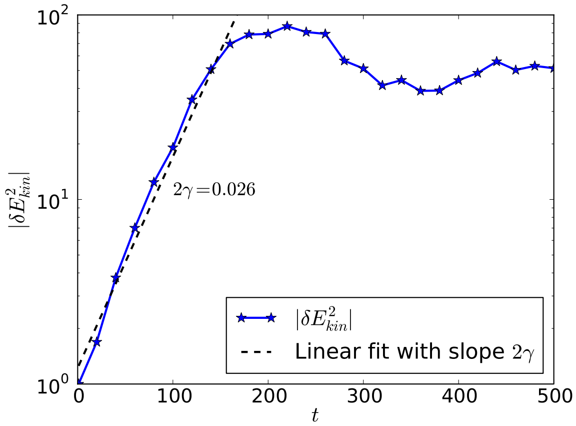

FIG. 2 (color online). Time evolution of perturbed kinetic energy along $\hat{y}$ [Eq. (2)] on a log-linear scale for $m_n = 4$ and $\Gamma = 25$. The dashed line shows a fit to the initial linear growth regime.

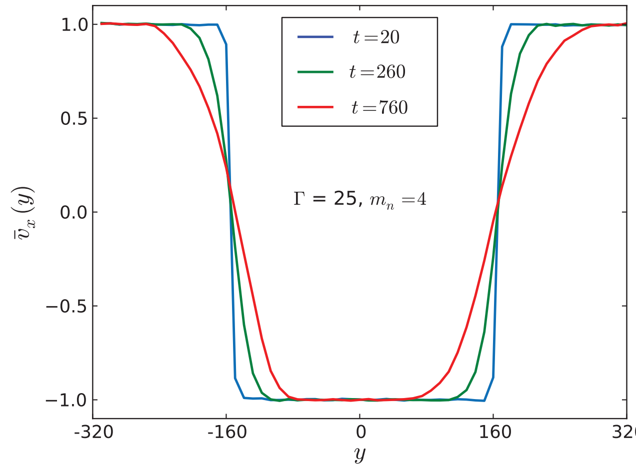

FIG. 3 (color). Time evolution of $\hat{x}$ independent velocity shear profile. System size $L = 640$.

to a Gaussian thermostat [22] and letting it evolve canonically for $250\omega_{\rm pd}^{-1}$. After this we remove the thermostat and let the system evolve for another $250\omega_{\rm pd}^{-1}$ microcanonically at the end of which it attains a thermal equilibrium corresponding to the desired Γ. A leapfrog integrator with a time step $\Delta t = 0.01$ is used such that the fluctuation in total energy without the thermostat is $<10^{-3}\%$ over an interval of $1000\omega_{\rm pd}^{-1}$.

Basic features of strong coupling.—In Fig. 1 we show the pair correlation function (PCF) $g(r)$ obtained by MD simulations, which contains strong coupling information of the system. At higher values of coupling parameter, amplitude of the peaks increase clearly indicating stronger coupling. The hydrodynamical limit of the problem corresponds to $\Gamma \to 1$, i.e., no peaks at all in $g(r)$.

Kelvin Helmholtz instability.—A shear flow U is then superposed on particle velocities along $\hat{x}$ which has the following form:

$$U = \begin{cases} +U_0[1 + \Delta\cos(k_x x)], & |y| \geq L/4, \\ -U_0[1 + \Delta\cos(k_x x)], & |y| < L/4, \end{cases} \tag{1}$$

where x, y are the components of the position vector of any particle, L is the size of the system centered at the origin $(0, 0)$, and U_0 is the magnitude of the shear velocity. In our normalized units $U_0 = 1$, amplitude of perturbation Δ is 0.1 and $k_x = 2\pi m_n/L$, where m_n is the mode number of perturbation. The sound speed computed for our system for the entire range of Γ varies between 1.5 to 1.6. Hence the flow speed U_0 is subsonic and our shear flow studies can be thought of as "incompressible" in nature. To understand the growth characteristic of a particular mode m_n we study the time evolution of the perturbed kinetic energy along $\hat{y}$ normalized to its initial value:

$$|\delta E^2_{\rm kin}| = \frac{\iint (v_y(t)^2 - v_y(0)^2)dxdy}{\iint v_y(0)^2 dxdy}. \tag{2}$$

Figure 2 shows the growth of this perturbed kinetic energy for $m_n = 4$ for an initial state $\Gamma = 25$ on a log-linear scale. It is clear from Fig. 2 that the logarithm of the perturbed kinetic energy grows linearly in time leading to nonlinear saturation at late times. The dashed line shows a linear fit to this linear growth regime. In Fig. 3, we show the time evolution of $\hat{x}$ independent flow velocity defined by $\bar{v}_x(y) = [1/L]\int_{-L/2}^{L/2} v_x dx$. At $t = 20$, $\bar{v}_x(y)$ has close to a double step profile. We then see a subsequent flattening of the step shear profile with time.

Comparison with hydrodynamics.—Analytic solution for the viscous growth rate in KH instability for a step

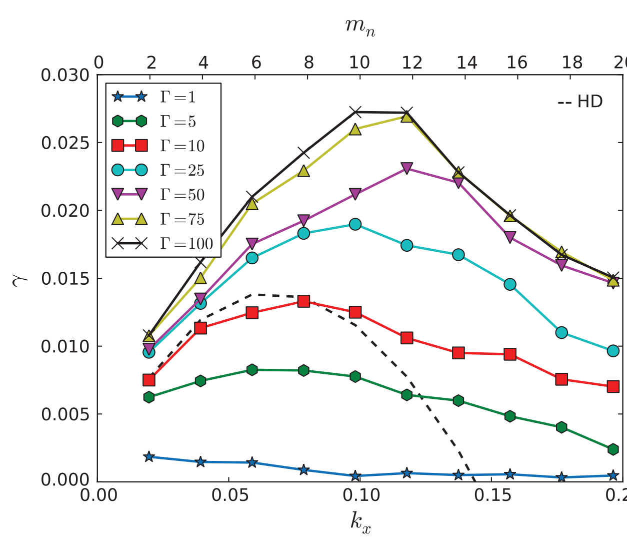

FIG. 4 (color). Growth rate spectra of KH instability calculated from MD. Each point on a given curve is obtained from the slope of the straight line fit to linear growth of perturbed kinetic energy. For comparison, the growth rates calculated from hydrodynamics (HD) [see Eq. (3)] at $R_E = 1$ is shown as the dashed line. Viscous stabilization is clearly seen at higher modes for all Γ.

shear profile is well known in hydrodynamics [23]. In our notation it reads as

$$\gamma = \frac{k_x U_0}{3}\left\{\sqrt{3} - 2\frac{k_x}{R_E} - 2\left[\left(\frac{k_x}{R_E}\right)^2 + 2\sqrt{3}\frac{k_x}{R_E}\right]^{1/2}\right\}, \quad (3)$$

where k_x is the dimensionless wave number and U_0 is the dimensionless shear velocity. The Reynolds number R_E is defined as $R_E = U_0 dn/\eta$, where d is the shearing length scale and η is the shear viscosity. Using equilibrium MD simulations [24] we calculate η for our system and find it to vary between 0.7 at $\Gamma = 1$ to 0.9 at $\Gamma = 100$ with a minimum ($\eta \approx 0.2$) close to $\Gamma \approx 30$. Our results for η are qualitatively similar to earlier works [25] (although with a different density n). Since the shearing length scale d is of the order of the interparticle distance, i.e., 1 and $n = 0.61$, the conventional Reynolds number for our problem is $R_E \approx 1$. In Fig. 4 growth rates γ (normalized to ω_{pd}) calculated directly from MD are plotted as a function of m_n for various values of initial Γ. For comparison the hydrodynamic growth rates calculated from Eq. (3) at $R_E = 1$ is shown as the dashed line. As can be expected, we observe viscous stabilization at higher modes for all Γ. From Fig. 4 it is clearly seen that growth rates at higher modes are much higher than those predicted by Eq. (3). We believe this is due to the presence of strong correlation effects which manifest themselves in not only viscosity, but also long range order (oscillations in PCF as seen in Fig. 1) and hence deviations from viscous hydrodynamics [Eq. (3)] can be expected. We also see that the maximum growth rates tend to saturate as Γ increases towards the solid regime. It will be interesting to study KH instability close to and across the liquid-solid regime ($\Gamma \approx 140$) but is beyond the scope of present work. It is interesting to note that at the weakest coupling studied, i.e., $\Gamma = 1$, MD growth rates are very small ($\approx 10^{-3}$). This happens because the ratio $U_0/v_{\mathrm{th}} \approx 0.71 < 1$. It should be noted that while U_0 is "streaming" in nature, the thermal velocity $v_{\mathrm{th}} = \sqrt{2/\Gamma}$ is "random." For growth rates to become significant U_0/v_{th} should be >1. It is clearly seen from Fig. 4 that the strong coupling effects increase the instability growth rates. (It should be noted that a single run of time interval $1000\omega_{\mathrm{pd}}^{-1}$ takes about 28 h on a 32 CPU parallel Linux cluster making it computationally expensive and Fig. 4 shows the linear growth rates computed from 70 such runs.) The development of KH instability leads to the formation of vortices which eventually leads to turbulent mixing of Yukawa liquid. Figure 5. shows the instantaneous snapshots of the particle coordinates to illustrate the formation of vortices. The particles are colored according to the initial shear velocity imposed on them [Eq. (1)]. A particle at time $t = 0$ (when the shear is imposed) is colored blue if $|y| \geq L/4$, else colored green. A given mode $m_n = 4$ is excited for four values of $\Gamma = 1$, 5, 25, 75 and instantaneous snapshots at three different times are taken for each Γ. One can easily notice that for higher values of Γ, the KH rolls at any given time are clearer and

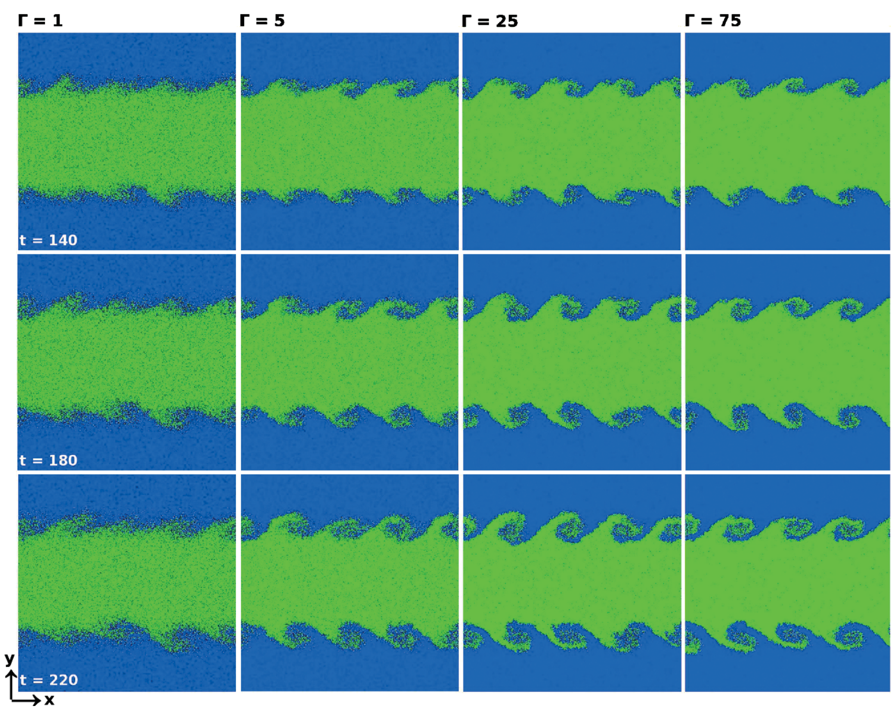

FIG. 5 (color). Blue colored fluid moves in the $+\hat{x}$ and green colored moves in $-\hat{x}$. The snapshots are shown for the full system ($\pm L/2$, $\pm L/2$) at times $t = 140$, 180, 220 for four different values of Γ namely $\Gamma = 1$, 5, 25, 75 when a given mode ($m_n = 4$) is excited. Horizontal and vertical rows show snapshots at constant t and Γ, respectively. At higher Γ's, the mode structures are more prominent. It is interesting to note that at the highest temperature $\Gamma = 1$, mode structures are weak and look diffusive due to high thermal agitation.

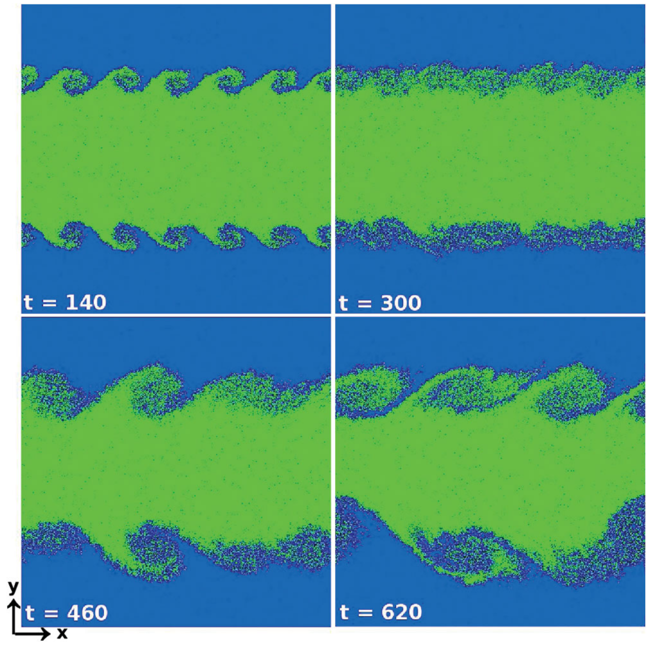

FIG. 6 (color). Inverse cascading of mode $m_n = 6$ starting from an initial state of $\Gamma = 50$. At $t = 140$, $m_n = 6$ appears eventually becoming $m_n = 3$ at $t = 460$. Snapshot at $t = 300$ shows an intermediate state when the initial mode $m_n = 6$ has already collapsed. Finally at $t = 620$, the definite features of mode structures are lost and the turbulent behavior of the liquid is qualitatively seen.

more pronounced. It is interesting to note that for $1 < \Gamma < 10$ ($U_0/v_{\rm th} \sim 0.7 - 2.3$) the collective effects are seen even at the particle level. In Fig. 6 we show the inverse cascading of the mode $m_n = 6$ in a Yukawa liquid at $\Gamma = 50$. At $t = 140$ the mode $m_n = 6$ (six rolls) appears which collapses at $t = 300$ before reemerging as $m_n = 3$ at $t = 460$. The snapshot at $t = 300$ shows the transition of m_n from $6 \rightarrow 3$. By $t = 620$, one can see that the well-defined mode structures are lost and the transition to turbulence is qualitatively seen. Using typical experimental parameters [10] $m \approx 4 \times 10^{-13}$ kg, $Q \approx 12\,000e$ where e is electronic charge and $a = 0.4$ mm we get $\omega_{\rm pd} \approx 50$ s^{-1}. A typical growth rate in our study $\gamma = 0.02\omega_{\rm pd}$ corresponds to approximately 1 s^{-1} in physical units and hence should be observable in laboratory experiments.

Summary.—We have observed Kelvin Helmholtz instability in strongly coupled Yukawa liquids at the particle level for the first time. A double step velocity shear profile is used to study this instability. The linear growth rates (γ) are directly computed from MD simulations and vortex-roll formation in the nonlinear regime is reported. The most interesting feature we notice here is the increase of instability growth rate with strong coupling. We also observe inverse cascading of the modes in time. Several open questions can be addressed in the context of the present work such as study of random perturbation (multiple m_n's), comparison to viscoelastic hydrodynamics [16], shock propagation (supersonic U_0), detailed study of transition to turbulence, instability across liquid-solid regime ($\Gamma \approx 140$), and study of flows with resonantly unstable modes [26], to name a few.

The work was carried out using the parallel code multi-potential molecular dynamics (MPMD) [7] developed by the authors at Institute for Plasma Research-Gandhinagar and run on Quad core Intel Linux cluster.

*ganesh@ipr.res.in

[1] Z. Donko, G. J. Kalman, and P. Hartmann, J. Phys. Condens. Matter **20**, 413101 (2008).
[2] G. E. Morfill and A. V. Ivlev, Rev. Mod. Phys. **81**, 1353 (2009).
[3] H. Thomas, G. E. Morfill, V. Demmel, J. Goree, B. Feuerbacher, and D. Möhlmann, Phys. Rev. Lett. **73**, 652 (1994).
[4] J. H. Chu and L. I, Phys. Rev. Lett. **72**, 4009 (1994).
[5] H. M. Thomas and G. Morfill, Nature (London) **379**, 806 (1996).
[6] S. Hamaguchi, R. T. Farouki, and D. H. E. Dubin, Phys. Rev. E **56**, 4671 (1997).
[7] Ashwin J. and R. Ganesh, Phys. Rev. E **80**, 056408 (2009).
[8] S. A. Khrapak, A. V. Ivlev, and G. E. Morfill, Phys. Rev. E **70**, 056405 (2004).
[9] G. E. Morfill, M. Rubin-Zuzic, H. Rothermel, A. V. Ivlev, B. A. Klumov, H. M. Thomas, U. Konopka, and V. Steinberg, Phys. Rev. Lett. **92**, 175004 (2004).
[10] V. Nosenko and J. Goree, Phys. Rev. Lett. **93**, 155004 (2004).
[11] N. D'Angelo and B. Song, Planet. Space Sci. **38**, 1577 (1990).
[12] G. T. Birk and H. Wiechen, Phys. Plasmas **9**, 964 (2002).
[13] H. M. Wiechen, Phys. Plasmas **13**, 062104 (2006).
[14] D. C. Montgomery and D. A. Tidman, *Plasma Kinetic Theory* (McGraw Hill Book Company, New York, 1964).
[15] S. Ichimaru, *Basic Principles of Plasma Physics: A Statistical Approach* (The Benjamin/Cummings Publishing Company, Inc., Reading, MA, 1973).
[16] P. K. Kaw and A. Sen, Phys. Plasmas **5**, 3552 (1998).
[17] *Strongly Coupled Plasmas* edited by Gabor J. Kalman and Paul Carini (Plenum Press, New York, 1977).
[18] *Strongly Coupled Coulomb Systems*, edited by Gabor J. Kalman, Martin P. Rommel, and Krastan B. Blagoev (Plenum Press, New York, 1998).
[19] K. Kadau, J. L. Barber, T. C. Germann, and B. J. Alder, Phys. Rev. E **78**, 045301(R) (2008).
[20] D. C. Rapaport, Phys. Rev. Lett. **60**, 2480 (1988).
[21] P. Hartmann, G. J. Kalman, Z. Donkó, and K. Kutasi, Phys. Rev. E **72**, 026409 (2005).
[22] D. J. Evans, J. Chem. Phys. **78**, 3297 (1983).
[23] P. Drazin, J. Fluid Mech. **10**, 571 (1961).
[24] T. Saigo and S. Hamaguchi, Phys. Plasmas **9**, 1210 (2002).
[25] B. Liu and J. Goree, Phys. Rev. Lett. **94**, 185002 (2005).
[26] S. Chandrasekhar, *Hydrodynamic and Hydromagnetic Stability* (Dover Publications, New York, 1998).